Int. J. Solids Structures Vol. 19, No. 2, pp. 165–177, 1982
Printed in Great Britain.

0020-7683/83/020165-13$03.00/0

APPLIED TRACTIONS ON THE SURFACE OF AN INFINITE CYLINDRICAL BORE

R. PARNES†
Laboratoire de Mécanique des Solides, Ecole Polytechnique, 91128 Palaiseau, France

(*Received* 15 *July* 1981)

Abstract—Applied tractions acting on the surface of a cylindrical bore in an infinite elastic medium are considered. The statically applied tractions are of the form of radial pressure and torsional circular line loads. Integral representations of the displacement and stress fields are derived and numerical results are presented showing the decay of the response with the distance from the point of load application. The results obtained represent long-time solutions for the corresponding dynamic problem as well as the limiting case of applied time-harmonic loadings as the frequency goes to zero.

1. INTRODUCTION

The problem of applied tractions acting on the surface of a bore in an elastic medium was considered many years ago. Among the first investigations were those of Westergaard [1] who studied the static response of an elastic medium to applied radial pressures acting over a finite length of the bore. However few numerical results, confined only to the bore surface, were presented, undoubtedly due to the lack of modern computing facilities existing at the time. Jordan [2] later treated the corresponding dynamic problem of a sudden application of pressure over a finite interval of the bore, but in view of the complexities encountered in this more difficult problem, presented numerical results only at large distances (i.e. 20 radii or more) away from the nearest point of load application.

In the present problem, the application of a traction acting statically on a circle of the cylindrical bore is considered. The application of circular line loads of this nature, expressed as Dirac-delta functions in the axial coordinate, has been used previously by the author in the investigation of the effect of moving loads [3, 4].

The line loads considered here are of two types: a statically applied radial pressure load and a torsional line load. Integral representations for the displacement and stress fields are obtained and numerical results are given for the displacement and stress components both along a radial line emanating from the load and along the bore surface. Curves showing the decay of these quantities with the distance from the point of load application indicate the degree of significant penetration into the medium which can be expected. Thus the static response, which has been largely neglected, is of interest (e.g. in the field of hydraulic fracture) since it reveals to some extent as a first approximation, the area of damage which may be encountered due to applied loads acting on the walls of existing bore holes. The static response is also of interest since it represents the long-time solution to problems of sudden load application and also the limiting case of time-harmonic prescribed loads as the frequency approaches zero. In addition, the solutions to the present problem of applied line loads can be considered as the Green's functions to evaluate the response due to applied loads having arbitrary axi-symmetric space variations along the bore surface.

2. GENERAL FORMULATION AND SOLUTION

Consider a cylindrical bore of radius $r = a$ in a linear isotropic elastic medium with shear modulus μ and Poisson ratio ν. The medium is referred to a non-dimensional cylindrical coordinate system ($\rho = r/a$, θ, $\xi = z/a$) whose origin lies at the center of the bore (Fig. 1). Axisymmetric line loads of intensity P, either radial pressure or torsional, act on the bore surface along a circle at $\xi = 0$.

†This investigation was performed while the author was on leave during 1980–1981 from Dept. of Solid Mechanics, Materials and Structures, School of Engineering, Tel-Aviv University, Ramat-Aviv, 69978 Tel-Aviv, Israel.

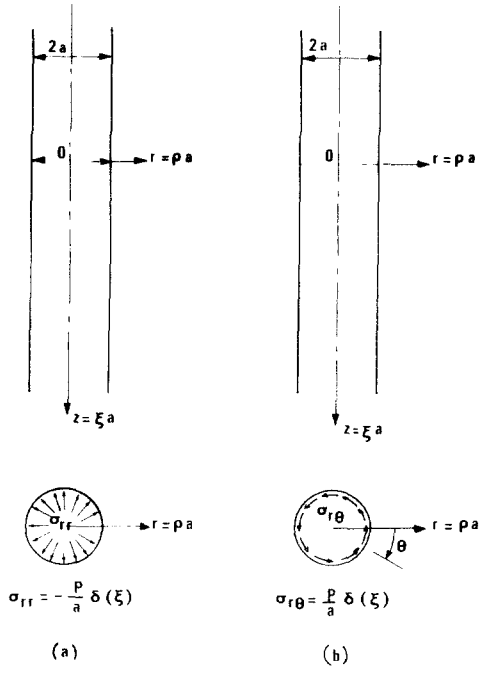

Fig. 1. Geometry of problem.

The boundary conditions are then either

$$\sigma_{rr} = -\frac{P}{a}\delta(\xi), \qquad \sigma_{rz} = \sigma_{r\theta} = 0, \qquad \rho = 1 \quad \text{(a)}$$

or (1)

$$\sigma_{r\theta} = \frac{P}{a}\delta(\xi), \qquad \sigma_{rr} = \sigma_{rz} = 0, \qquad \rho = 1 \quad \text{(b)}$$

where $\delta(\xi)$ is the Dirac-delta function.

The displacements

$$\tilde{u}(\rho, \xi) = w\tilde{k}_r + v\tilde{k}_\theta + u\tilde{k}_z \tag{2}$$

must satisfy the equilibrium equations

$$\mu\nabla^2\tilde{u} + (\lambda + u)\nabla\nabla \cdot \tilde{u} = 0 \tag{3}$$

where

$$\nabla = \frac{\partial}{\partial\rho}\tilde{k}_r + \frac{1}{\rho}\frac{\partial}{\partial\theta}\tilde{k}_\theta + \frac{\partial}{\partial\xi}\tilde{k}_z. \tag{4}$$

Since the method of solution for the radial and torsional loads differ, each will be treated separately.

(a) *Axi-symmetric radial solution*

For this case the circumferential displacement $v = 0$. The behavior of the medium can then be readily formulated in terms of a Love strain function $\phi(\rho, \xi)$ [5]. Expressing the non-vanishing radial and axial displacements for this axi-symmetric case by

$$w = -\frac{1}{2\mu a^2}\frac{\partial^2\phi}{\partial\rho\partial\xi} \tag{5a}$$

$$u = \frac{1}{a^2}\left[\frac{1-\nu}{\mu}\nabla^2\phi - \frac{1}{2\mu}\frac{\partial^2\phi}{\partial\xi^2}\right] \tag{5b}$$

respectively, the equation of equilibrium, eqn (3), is satisfied if

$$\nabla^4\phi(\rho, \xi) = 0. \tag{6}$$

Appropriate solutions of the bi-harmonic equation which decay as $\rho \to \infty$ are [6]

$$\phi(\rho, \xi) = \int_0^\infty f(\rho) \sin \alpha\xi \, d\alpha \tag{7a}$$

where

$$f(\rho) = A(\alpha)K_0(\alpha\rho) + B(\alpha)\rho K_1(\alpha\rho). \tag{7b}$$

In the above, $K_n(\alpha\rho)$ are the modified Bessel functions of order n, and $A(\alpha)$ and $B(\alpha)$ are undetermined constants.

The stress components expressed in terms of the potential function $\phi(\rho, \xi)$ are: [5]

$$\left.\begin{aligned}
\sigma_{rr}(\rho, \xi) &= \frac{1}{a^3}\frac{\partial}{\partial\xi}\left[\nu\nabla^2\phi - \frac{\partial^2\phi}{\partial\rho^2}\right] \\
\sigma_{\theta\theta}(\rho, \xi) &= \frac{1}{a^3}\frac{\partial}{\partial\xi}\left[\nu\nabla^2\phi - \frac{1}{\rho}\frac{\partial\phi}{\partial\rho}\right] \\
\sigma_{zz}(\rho, \xi) &= \frac{1}{a^3}\frac{\partial}{\partial\xi}\left[(2-\nu)\nabla^2\phi - \frac{\partial^2\phi}{\partial\xi^2}\right] \\
\sigma_{rz}(\rho, \xi) &= \frac{1}{a^3}\frac{\partial}{\partial\rho}\left[(1-\nu)\nabla^2\phi - \frac{\partial^2\phi}{\partial\xi^2}\right] \\
\sigma_{r\theta} &= \sigma_{\theta z} = 0.
\end{aligned}\right\} \tag{8}$$

The boundary conditions for the axial radial case, eqn (1a), then become

$$\left.\begin{aligned}
\frac{\partial}{\partial\xi}\left[\nu\nabla^2\phi - \frac{\partial^2\phi}{\partial\rho^2}\right]\Bigg|_{\rho=1} &= -\frac{Pa^2}{\pi}\int_0^\infty \cos\alpha\xi \, d\alpha \\
\frac{\partial}{\partial\rho}\left[(1-\nu)\nabla^2\phi - \frac{\partial^2\phi}{\partial\xi^2}\right]\Bigg|_{\rho=1} &= 0
\end{aligned}\right\} \tag{9}$$

where the Dirac-delta function has been replaced by the integral representation [7]

$$\delta(\xi) = \frac{1}{\pi}\int_0^\infty \cos\alpha\xi \, d\alpha. \tag{10}$$

It is noted that the last of the boundary conditions of eqn (1a) is satisfied identically.

Substituting $\phi(\rho, \xi)$ given by eqns (7a, b) in eqns (9), using the standard relations for the derivatives of the K_n functions [8], and equating term by term, results, after some manipulation, in the following equations for A and B:

$$\begin{bmatrix} \alpha K_0 + K_1 & (2\nu-1)K_0 + \alpha K_1 \\ -\alpha K_1 & -\alpha K_0 + 2(1-\nu)K_1 \end{bmatrix}\begin{Bmatrix} A \\ B \end{Bmatrix} = \begin{Bmatrix} \frac{a^2 P}{\pi\alpha^2} \\ 0 \end{Bmatrix}. \tag{11}\dagger$$

†For simplification, the following notation is used here and below: $K_n \equiv K_n(\alpha)$.

Solving the above system, the constants are determined:

$$A(\alpha) = \frac{Pa^2}{\pi D\alpha^2}[2(1-\nu)K_1 - \alpha K_0]$$
$$B(\alpha) = \frac{Pa^2}{\pi D\alpha}K_1 \tag{12}$$

where

$$D = 2(1-\nu)K_1^2 + \alpha^2(K_1^2 - K_0^2). \tag{13}$$

The displacement and stress components in the medium are then immediately obtained from eqns (5) and (8) in a non-dimensional form:

$$\frac{\mu w}{P} = \frac{1}{2\pi}\int_0^\infty \frac{1}{D}[\rho\alpha K_1K_0(\alpha\rho) + 2(1-\nu)K_1K_1(\alpha\rho) - \alpha K_0K_1(\alpha\rho)]\cos\alpha\xi\,d\alpha \tag{14a}$$

$$\frac{\mu u}{P} = \frac{1}{2\pi}\int_0^\infty \frac{1}{D}[\rho\alpha K_1K_1(\alpha\rho) - 2(1-\nu)K_1K_0(\alpha\rho) - \alpha K_0K_0(\alpha\rho)]\sin\alpha\xi\,d\alpha \tag{14b}$$

$$\frac{a\sigma_{rr}}{P} = \frac{1}{\pi}\int_0^\infty \frac{1}{D}\Big[\alpha^2K_0K_0(\alpha\rho) + \frac{\alpha}{\rho}K_0K_1(\alpha\rho) - \alpha K_1K_0(\alpha\rho) - [2(1-\nu)/\rho + \alpha^2\rho]K_1K_1(\alpha\rho)]\cos\alpha\xi\,d\alpha \tag{14c}$$

$$\frac{a\sigma_{\theta\theta}}{P} = \frac{1}{\pi}\int_0^\infty \frac{1}{D}\Big[-\frac{\alpha}{\rho}K_0K_1(\alpha\rho) + \frac{2(1-\nu)}{\rho}K_1K_1(\alpha\rho) + (1-2\nu)\alpha K_1K_0(\alpha\rho)\Big]\cos\alpha\xi\,d\alpha \tag{14d}$$

$$\frac{a\sigma_{zz}}{P} = \frac{1}{\pi}\int_0^\infty \frac{\alpha}{D}[\rho\alpha K_1K_1(\alpha\rho) - 2K_1K_0(\alpha\rho) - \alpha K_0K_0(\alpha\rho)]\cos\alpha\xi\,d\alpha \tag{14e}$$

$$\frac{a\sigma_{rz}}{P} = \frac{1}{\pi}\int_0^\infty \frac{\alpha^2}{D}[K_0K_1(\alpha\rho) - \rho K_1K_0(\alpha\rho)]\sin\alpha\xi\,d\alpha. \tag{14f}$$

The solution for the axi-symmetric radial case is formally complete. Evaluation of the above integrals and numerical results are given in the next section.

(b) *Axi-symmetric torsional solution*

For this case, the equation of equilibrium must be satisfied together with the boundary conditions, eqns (1b). Appropriate solutions satisfying eqn (3) are $\tilde{u} = v\tilde{k}_\theta$ with $u = w = 0$. The equation of equilibrium then reduces to the scalar equation

$$\frac{\partial^2 v}{\partial\rho^2} + \frac{1}{\rho}\frac{\partial v}{\partial\rho} - \frac{v}{\rho^2} + \frac{\partial^2 v}{\partial\xi^2} = 0. \tag{15}$$

The stresses, obtained from the stress–strain relations

$$\tilde{\sigma} = \frac{1}{a}\{\lambda\nabla\cdot\tilde{u}I + \mu[\nabla\tilde{u} + \tilde{u}\nabla]\} \tag{16}$$

become

$$\left.\begin{aligned} \sigma_{r\theta} &= \frac{\mu}{a}\Big(\frac{\partial v}{\partial\rho} - \frac{v}{\rho}\Big) && \text{(a)}\\ \sigma_{\theta z} &= \frac{\mu}{a}\frac{\partial v}{\partial\xi} && \text{(b)}\\ \sigma_{rr} &= \sigma_{\theta\theta} = \sigma_{rz} = \sigma_{zz} = 0. && \text{(c)} \end{aligned}\right\} \tag{17}$$

The last two boundary conditions of eqn (1b) are identically satisfied while, using eqn (17a), the remaining boundary condition is expressed as

$$\left.\frac{\partial v}{\partial \rho} - \frac{v}{\rho}\right|_{\rho=1} = \frac{P}{\mu\pi}\int_0^\infty \cos \alpha\xi \, d\alpha. \tag{18}$$

Again, the integral representation for the Dirac-delta function, eqn (10), has been used in eqn (18).

Appropriate solutions to eqn (15) which decay as $\rho \to \infty$ are given by

$$v(\rho, \xi) = \int_0^\infty C(\alpha) K_1(\alpha\rho) \cos \alpha\xi \, d\alpha. \tag{19}$$

Substituting in eqn (18), as before, and equating term by term, we obtain:

$$C(\alpha) = -\frac{P}{\mu\pi} \cdot \frac{1}{\alpha K_2(\alpha)} \tag{20}$$

and hence the displacement becomes

$$v(\rho, \xi) = -\frac{P}{\pi\mu}\int_0^\infty \frac{K_1(\alpha\rho)}{\alpha K_2(\alpha)} \cos \alpha\xi \, d\alpha. \tag{21a}$$

Substitution in eqns (17a, b) yields the following expressions for the non-vanishing stress components

$$\frac{a\sigma_{r\theta}}{P}(\rho, \xi) = \frac{1}{\pi}\int_0^\infty \frac{K_2(\alpha\rho)}{K_2(\alpha)} \cos \alpha\xi \, d\alpha \tag{21b}$$

$$\frac{a\sigma_{\theta z}}{P}(\rho, \xi) = \frac{1}{\pi}\int_0^\infty \frac{K_1(\alpha\rho)}{K_2(\alpha)} \sin \alpha\xi \, d\alpha. \tag{21c}$$

It is of interest to note that the above solution represents the degenerate case of a moving load system given by eqns (64) of [4]† (when q appearing in those equations is set to unity).

3. NUMERICAL SOLUTION AND RESULTS

The response to the axi-symmetric radial and torsional loadings are expressed by the integral representations of eqns (14) and (21) respectively. Due to the nature of the integrands, the integrals are integrated numerically. (Any attempt to integrate in the complex plane would eventually lead, in any case, to a numerical integration of the resulting branch integrals which arise due to the multivalued character of the modified Bessel functions.)

In general, the integrals are well-behaved and tend to zero as $\alpha \to \infty$. (Noting that $K_1 > K_0$, it follows that D appearing in the integrands of eqn (14) is always positive; consequently no singularities exist in $0 < \alpha < \infty$.) Moreover, all apparent singularities existing at $\alpha = 0$ are removable. We denote the integrands of the various quantities of eqns (14) by $Q_{(\,)}$. Upon representing the K_n functions by their power series [8], the following limits are obtained as $\alpha \to 0$:

$$\left.\begin{aligned} Q_w = 1/2\rho, \quad Q_{rr} = -1/\rho^2, \quad Q_{\theta\theta} = 1/\rho^2 \\ Q_u = Q_{zz} = Q_{rz} = 0. \end{aligned}\right\} \tag{22}$$

It is of interest to note that these values, as they necessarily must, correspond to the response to a constant traction $\sigma_{rr} = -1$ applied uniformly along the bore surface, $\rho = 1$, i.e. the classical Lamé problem [9].

†It is noted that a misprint appears in eqn (64a) of [4]; ω should appear in the denominator of the integrand.

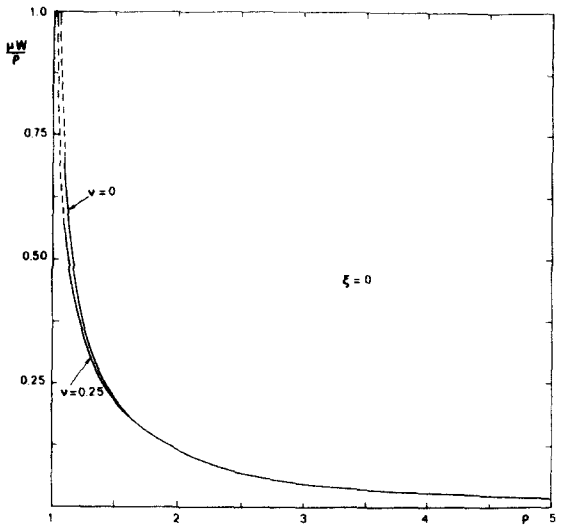

Fig. 2. Radial displacement along line $\xi = 0$ due to radial pressure load.

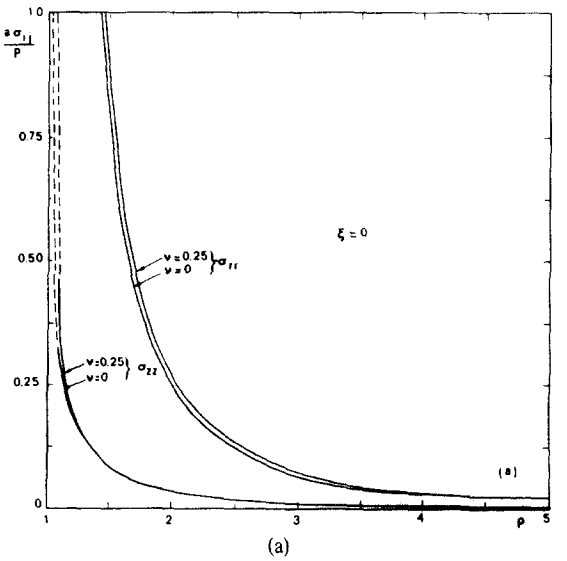

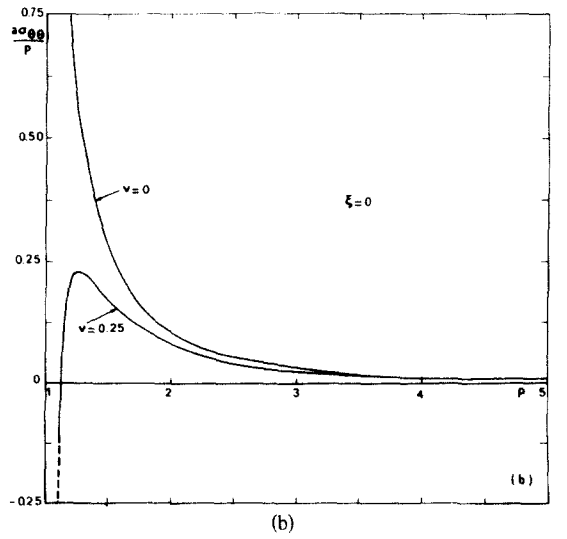

Fig. 3. Stress components along line $\xi = 0$ due to radial pressure load.

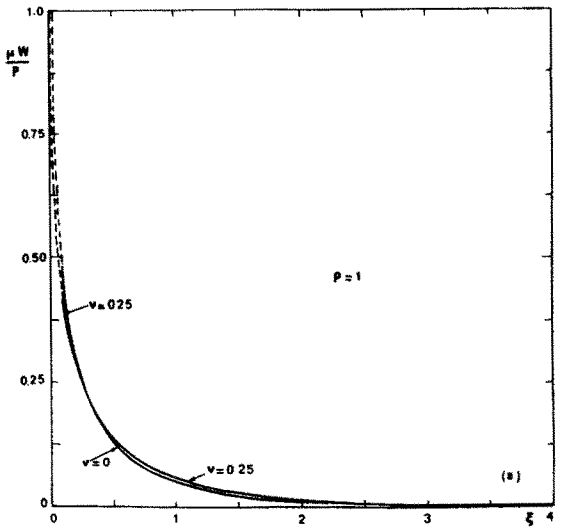

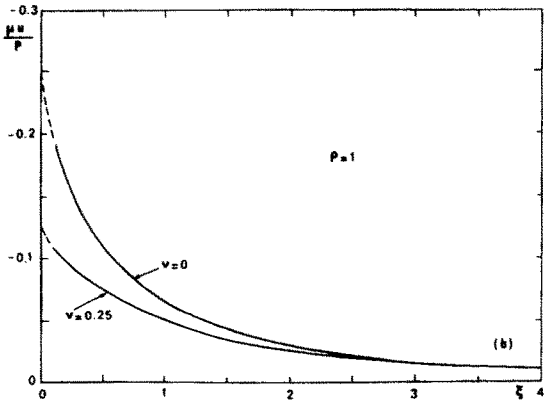

Fig. 4. Displacement components at bore surface due to radial pressure load.

Similarly the limiting values as $\alpha \to 0$ of the integrands of eqns (21) for the torsional loading case are found to be:

$$Q_v = -1/2\rho, \quad Q_{r\theta} = 1/\rho^2, \quad Q_{z\theta} = 0. \tag{23}$$

These values, which correspond to the response of a constant traction $\sigma_{r\theta} = 1$ applied uniformly along the surface $\rho = 1$, are given in [4].

Convergence of the integrals as $\alpha \to \infty$ and the method of integration are discussed in the Appendix.

(a) *Results: axi-symmetric radial loading*

Numerical results for this case are shown in Figs. 2–5. The curves presented were calculated using a value of $\alpha_0 = 60$ and increments, $\Delta\alpha = 0.025$. A verification of the method was established by using various values of similar order for α_0 and $\Delta\alpha$. In all cases, for values of $\rho > 1.1$, the same results were obtained to three significant figures. In the curves presented, results are given for two values of ν: $\nu = 0$ and 0.25.

In Fig. 2, the radial displacement w along the radial line $\xi = 0$ is presented as a function of ρ. It is seen that the displacement decays rapidly as ρ increases and, moreover, is not very sensitive to ν. Values are shown for $\rho > 1.1$ and suggested curves in the vicinity of the applied load

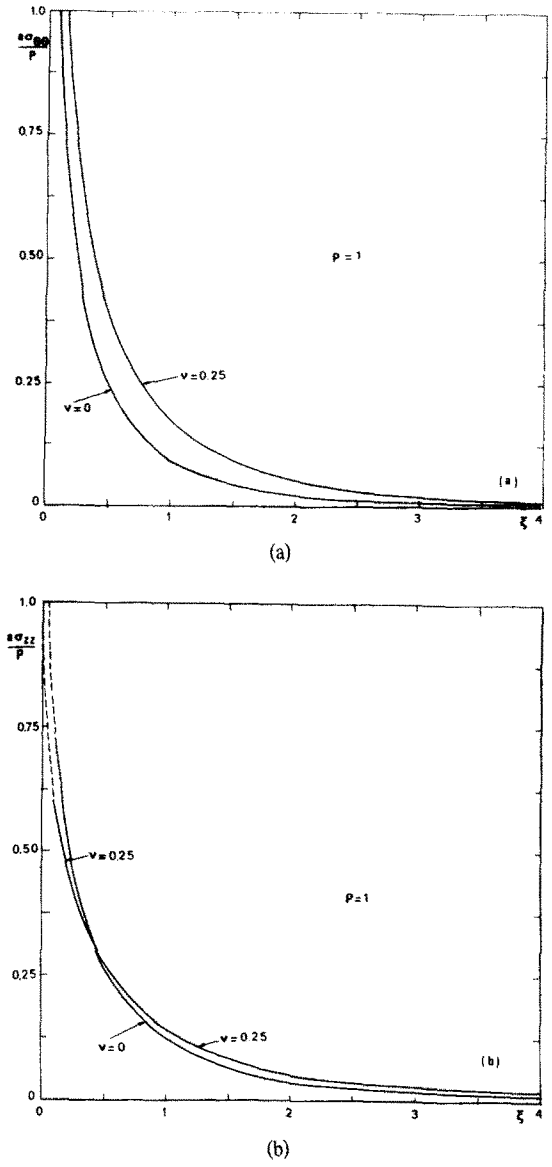

Fig. 5. Stress components at bore surface due to radial pressure load.

are indicated by broken lines.† It is clear that due to the nature of the Dirac-delta loading, the displacement near the point of load application becomes singular.

The variations of stress components σ_{rr} and σ_{zz} along the radial line $\xi = 0$ are shown in Fig. 3(a). Again, it is seen that the effect of Poisson's ratio on these stress components is quite small. However, from Fig. 3(b) we observe that as ρ approaches unity the stress component $\sigma_{\theta\theta}$ is particularly sensitive to ν. For $\nu = 0$, $\sigma_{\theta\theta}$ is seen to approach ∞ as $\rho \to 1$ while for $\nu = 0.25$ the limiting value becomes negative (and at a faster rate) as $\rho \to 1$. This result was found to be true for all values $\nu > 0$.

The response along the bore surface is shown in Figs. 4 and 5 as a function of ξ. We note, from Fig. 4(a), that the radial displacement w is very large near the point of load application, reflecting a singularity, and decays rapidly as ξ becomes large. Near the point of loading the displacement is greater for $\nu = 0$ than for $\nu = 0.25$ while the opposite is true for larger ξ.

†Near the point of loading, $\rho \lesssim 1.1$ and $\xi \lesssim 0.1$, the integration scheme described in the Appendix does not yield the desired accuracy (when using reasonable values of α_0 and $\Delta\alpha$) due to the existence of singularities in this region. (This is reflected by the slow decay of the integrals appearing in eqn (A17).) Consequently, the response in this region is shown in all figures by means of broken lines.

The longitudinal displacement u of the bore surface is presented in Fig. 4(b). Here we observe that, while decaying with increasing values of ξ, u does not become singular as $\xi \to 0$ but instead approaches a finite value dependent on ν. This would appear to represent a contradiction with the fact that $u(\xi = 0) = 0$, as seen in eqn (14b) and as must be true using conventional arguments of symmetry. However, this contradiction disappears if u is discontinuous at $\xi = 0$, namely if $\lim_{\xi \to 0} u(\xi) \neq u(0)$. We therefore conclude that a jump $[u]$ occurs at $\xi = 0$.†

In Figs. 5, the variations of the non-vanishing stress components $\sigma_{\theta\theta}$ and σ_{zz} acting at the bore surface are surface are shown. In both cases, the stresses are seen to be singular as $\xi \to 0$ and decay rapidly with increasing ξ.

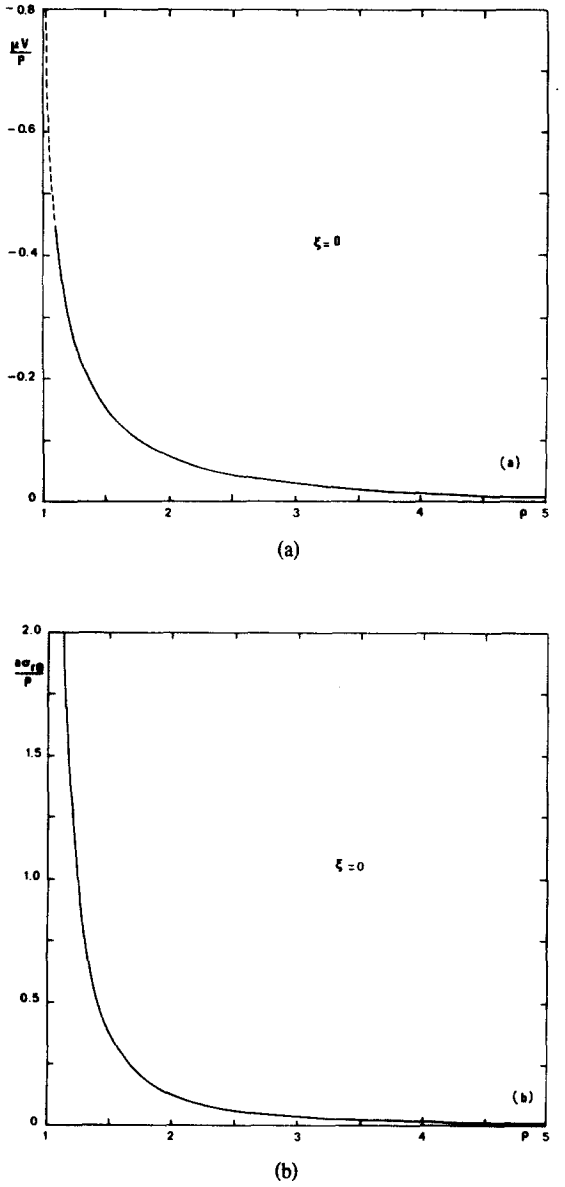

Fig. 6. Displacement and stress components along line $\xi = 0$ due to torsional load.

†A jump discontinuity in the displacement perpendicular to the applied load is known to occur when a concentrated load is applied and, in particular, when a concentrated line load, as in the present case, acts; for example, a half-space subjected to a normal circular line-load [10]. This phenomenon repeats itself in the corresponding dynamic problem [11].

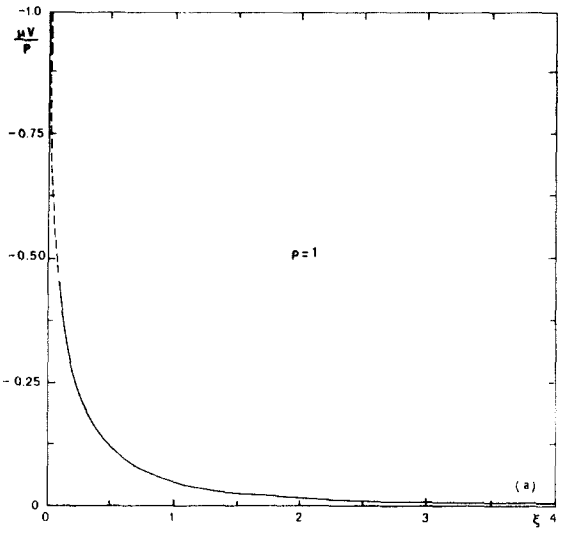

(a)

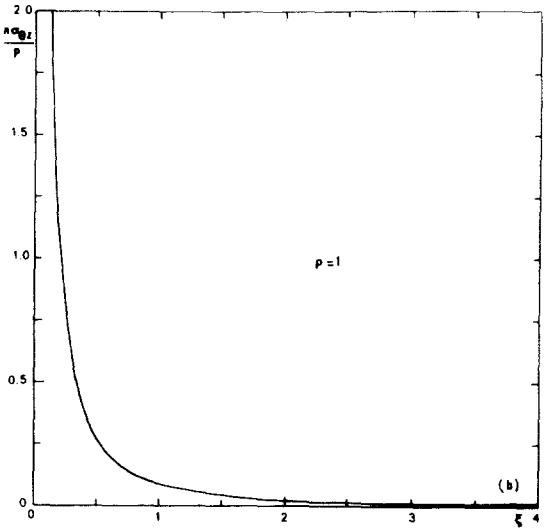

(b)

Fig. 7. Displacement and stress components at bore surface due to torsional load.

(b) *Results: torsional loading*

Results for the case of torsional loading are presented in Figs. 6 and 7. In Fig. 6(a), the variation of the circumferential displacement v along the radial line $\xi = 0$ is shown. The displacement is seen to decay monotonically with the radial parameter ρ. The non-vanishing stress $\sigma_{r\theta}$ is observed in Fig. 6(b) to decay rapidly in a similar manner.

The displacement v and stress component $\sigma_{\theta z}$ at the bore surface are shown in Fig. 7(a–b) respectively. Again, these quantities decay rapidly away from the point of load application.

4. CONCLUSION

The displacement and stress components are observed, for both loading cases (with the exception of $\sigma_{\theta\theta}$ when $\nu > 0$), to decay rapidly and monotonically with the distance from the point of load application. Disregarding the singularities existing at this point, we note that all quantities decay within a distance of $r = 2a$ and $r = 3a$ to the order of 8 and 3% respectively of their values at $r = 1.1a$. Hence we may conclude, that the effective penetration of the response is confined mainly to a zone within a radius $r \sim 2a$. Thus the effect beyond this range may be

considered as negligible. It follows, then, that the results of this study may be applied with small error to hollow tubes subjected to similar loads on the interior surface, $r = a$, provided that the outer radius $R > 3a$.

REFERENCES

1. H. M. Westergaard, *Karman Anniversary Volume* (1941).
2. D. W. Jordan, The stress wave from a finite cylindrical explosive source. *J. Math. Mech.* **11**, 503–551 (1962).
3. R. Parnes, Response of an infinite elastic medium to travelling loads in a cylindrical bore. *J. App. Mech.* **36**, 51–58 (1969).
4. R. Parnes, Progressing torsional loads along a bore in an elastic medium. *Int. J. Solids Structures* **16**, 653–670 (1980).
5. Y. C. Fung, *Foundations of Solid Mechanics*. Prentice-Hall, Englewood Cliffs, New Jersey (1965).
6. C.-S. Yih, Solutions of the hyper-bessel equation. *Q Appl. Math.* **13**, 462–463 (1956).
7. I. N. Sneddon, *Fourier Transforms*. McGraw-Hill, New York (1951).
8. N. W. McLachlan, *Bessel Functions for Engineers*. Oxford (1955).
9. S. Timosenko and J. Goodier, *Theory of Elasticity*, 2nd Ed., McGraw-Hill, New York (1951).
10. R. Parnes and E. R. Johnson, Axi-symmetric loads on an elastic half-space containing an inclusion. *Int. J. Engng Sci.* **11**, 717–724 (1973).
11. R. Parnes and E. R. Johnson, Propagation of axisymmetric waves in an elastic half-space containing a cylindrical inclusion—II. Analysis of singularities, behavior at wave fronts and numerical results. *Q J. Mech. Appl. Math.* **30**, Part 3, 255–268.
12. I. S. Gradshteyn and I. M. Ryzhik, *Table of Integrals, Series and Products*. Academic Press, New York (1965).
13. M. Abramowitz and I. A. Stegun (Eds), *Handbook of Mathematical Functions*. Dover, New York (1965).

APPENDIX

Evaluation of the integrals appearing in eqns (14) *and* (21)

The integrals appearing in eqns (14) and (21) must be integrated over the infinite domain $0 \leqslant \alpha < \infty$. The method of integration used is as follows: a prescribed value of α, $\alpha = \alpha_0$, is chosen such that the infinite domain is separated into two regions: $0 \leqslant \alpha \leqslant \alpha_0$ and $\alpha_0 \leqslant \alpha < \infty$. In the first region, the integrals are integrated by an appropriate numerical scheme (e.g. Simpson's rule) and the resulting integral for each desired quantity is represented by $S^{(1)}_{(\,)}$; i.e.

$$S^{(1)}_{(\,)} = \int_0^{\alpha_0} Q_{(\,)}(\alpha) \begin{Bmatrix} \cos \alpha\xi \\ \sin \alpha\xi \end{Bmatrix} \mathrm{d}\alpha \tag{A1}$$

where $Q_{(\,)}(\alpha)$ denotes the appropriate integrand for the displacement or stress component.

The remaining integral is denoted by $S^{(2)}_{(\,)}$; i.e.

$$S_{(\,)} = \frac{1}{\pi} \int_0^{\infty} Q_{(\,)}(\alpha) \begin{Bmatrix} \cos \alpha\xi \\ \sin \alpha\xi \end{Bmatrix} \mathrm{d}\alpha. \tag{A2a}$$

The total integral

$$S_{(\,)} = \frac{1}{\pi} \int_0^{\infty} Q_{(\,)}(\alpha) \begin{Bmatrix} \cos \alpha\xi \\ \sin \alpha\xi \end{Bmatrix} \mathrm{d}\alpha \tag{A2b}$$

is then

$$S_{(\,)} = \frac{1}{\pi} [S^{(1)}_{(\,)} + S^{(2)}_{(\,)}]. \tag{A3}$$

If α_0 is chosen sufficiently large, then $K_n(x)$ appearing in the integrands Q of $S^{(2)}$, can be represented by their asymptotic expansion [8]

$$K_n(x) \sim \sqrt{(\pi/2x)}\, \mathrm{e}^{-x} [1 + a_n/x + b_n/x^2 + \cdots] \tag{A4a}$$

where

$$a_n = \frac{4n^2 - 1}{8}, \quad b_n = \frac{(4n^2 - 1)(4n^2 - 9)}{128}. \tag{A4b}$$

Using these asymptotic expansions and retaining the first terms, the asymptotic representations of $Q(\alpha)$ are immediately determined and the integrals $S^{(2)}$ may then be evaluated analytically.

Substituting eqns (A4) in eqns (14) results upon taking the leading terms, in the following expressions for $S^{(2)}$ for the case of the axi-symmetric radial loads:

$$S^{(2)}_w = \begin{cases} \rho^{-1/2}(\rho - 1)/2 \displaystyle\int_{\alpha_0}^{\infty} \mathrm{e}^{-\alpha(\rho-1)} \cos \alpha\xi \, \mathrm{d}\alpha & \rho > 1 \quad \text{(A5a)} \\ (1 - \nu) \displaystyle\int_{\alpha_0}^{\infty} \frac{\cos \alpha\xi}{\alpha} \mathrm{d}\alpha & \rho = 1 \quad \text{(A5b)} \end{cases}$$

$$S_u^{(2)} = \begin{cases} \rho^{1/2}(\rho-1)/2 \int_{\alpha_0}^{\infty} e^{-\alpha(\rho-1)} \sin \alpha\xi \, d\alpha & \rho > 1 \quad \text{(A6a)} \\ -\dfrac{(1-2\nu)}{2} \int_{\alpha_0}^{\infty} \dfrac{\sin \alpha\xi}{\alpha} d\alpha & \rho = 1 \quad \text{(A6b)} \end{cases}$$

$$S_{rr}^{(2)} = \begin{cases} -\rho^{-1/2}(\rho-1) \int_{\alpha_0}^{\infty} \alpha \, e^{-\alpha(\rho-1)} \cos \alpha\xi \, d\alpha & \rho > 1 \quad \text{(A7a)} \\ -\int_{\alpha_0}^{\infty} \cos \alpha\xi \, d\alpha & \rho = 1 \quad \text{(A7b)} \end{cases}$$

$$S_{\theta\theta}^{(2)} = \begin{cases} \rho^{-1/2}[1 - 1/\rho - 2\nu] \int_{\alpha_0}^{\infty} e^{-(\rho-1)\alpha} \cos \alpha\xi \, d\alpha & \rho > 1 \quad \text{(A8a)} \\ -2\nu \int_{\alpha_0}^{\infty} \cos \alpha\xi \, d\alpha & \rho = 1 \quad \text{(A8b)} \end{cases}$$

$$S_{zz}^{(2)} = \begin{cases} \rho^{-1/2}(\rho-1) \int_{\alpha_0}^{\infty} \alpha \, e^{-(\rho-1)\alpha} \cos \alpha\xi \, d\alpha & \rho > 1 \quad \text{(A9a)} \\ -\int_{\alpha_0}^{\infty} \cos \alpha\xi \, d\alpha & \rho = 1 \quad \text{(A9b)} \end{cases}$$

$$S_{rz}^{(2)} = \begin{cases} -\rho^{-1/2}(\rho-1) \int_{\alpha_0}^{\infty} \alpha \, e^{-(\rho-1)\alpha} \sin \alpha\xi \, d\alpha & \rho > 1 \quad \text{(A10a)} \\ 0 & \rho = 1. \quad \text{(A10b)} \end{cases}$$

It is noted that eqns (A7b) and (A10b) reflect the given boundary conditions of eqn (1a) at $\rho = 1$ and thus are a confirmation of the correctness of the derived expressions. However, the expressions for $S_{\theta\theta}^{(2)}$ and $S_{zz}^{(2)}$, eqns (A8b) and (A9b), appear as divergent integrals when $\rho = 1$. Noting that for $\alpha > \alpha_0$, their form is identical to the representation of the Dirac-delta function given by eqn (10), it is possible to eliminate this divergence using the following procedure. We denote non-trigonometric part of the integrands of $\sigma_{\theta\theta}$ and σ_{zz} appearing in eqns (14d, e) by Q_{ij}, and let

$$\beta_{ij} = \lim_{\alpha \to \infty} Q_{ij}(\alpha)|_{\rho=1}. \quad \text{(A11)}$$

Upon taking the limit,

$$\beta_{\theta\theta} = -2\nu \quad \text{and} \quad \beta_{zz} = -1. \quad \text{(A12a, b)}$$

The integral representation of σ_{ij} may then be written as

$$\left.\frac{a\sigma_{ij}}{P}\right|_{\rho=1} = \frac{1}{\pi}\int_0^{\infty} Q_{ij}|_{\rho=1} \cos \alpha\xi \, d\alpha = \frac{\beta_{ij}}{\pi}\int_0^{\infty} \cos \alpha\xi \, d\alpha + \frac{1}{\pi}\left\{\int_0^{\alpha_0} (Q_{ij}|_{\rho=1} - \beta_{ij}) \cos \alpha\xi \, d\alpha + \int_{\alpha_0}^{\infty} (Q_{ij}|_{\rho=1} - \beta_{ij}) \cos \alpha\xi \, d\alpha\right\}. \quad \text{(A13)}$$

The first right-hand term is recognized as representing $\beta_{ij}\delta(\xi)$ and the second term, denoted now as

$$S_{ij}^{(1)} = \frac{1}{\pi}\int_0^{\alpha_0} (Q_{ij}|_{\rho=1} - \beta_{ij}) \cos \alpha\xi \, d\alpha \quad \text{(A14)}$$

is integrated numerically. Retaining higher order terms of the asymptotic expansion, eqn (A4) and proceeding as previously, the last integrals of eqn (A13) denoted as $S_{(\,)}^{(2)}$ become

$$\left.\begin{aligned} S_{\theta\theta}^{(2)}|_{\rho=1} &= -(2 - 3\nu/2) \int_{\alpha_0}^{\infty} \frac{\cos \alpha\xi}{\alpha} d\alpha \\ S_{zz}^{(2)}|_{\rho=1} &= -3/4 \int_{\alpha_0}^{\infty} \frac{\cos \alpha\xi}{\alpha} d\alpha. \end{aligned}\right\} \quad \text{(A15)}$$

Thus, *in lieu* of eqn (A3), $\sigma_{\theta\theta}$ and σ_{zz} at the bore surface, are expressed as

$$\left.\frac{a\sigma_{ij}}{P}\right|_{\rho=1} = \beta_{ij}\delta(\xi) + \frac{1}{\pi}[S_{ij}^{(1)} + S_{ij}^{(2)}]. \quad \text{(A16)}$$

The integrals of eqns (A5a)–(A10a) may be readily integrated in the case of $\rho > 1$. The final results are [12]:

$$\int_{\alpha_0}^{\infty} e^{-\alpha(\rho-1)} \begin{Bmatrix} \cos \alpha\xi \\ \sin \alpha\xi \end{Bmatrix} d\alpha = \frac{e^{-(\rho-1)\alpha_0}}{h} \left[\pm\xi \begin{Bmatrix} \sin(\alpha_0\xi) \\ \cos(\alpha_0\xi) \end{Bmatrix} - (\rho-1) \begin{Bmatrix} \cos(\alpha_0\xi) \\ \sin(\alpha_0\xi) \end{Bmatrix} \right] \tag{A17a}$$

$$\int_{\alpha_0}^{\infty} \alpha\, e^{-\alpha(\rho-1)} \begin{Bmatrix} \cos \alpha\xi \\ \sin \alpha\xi \end{Bmatrix} d\alpha = -\frac{e^{-(\rho-1)\alpha_0}}{h} \left\{ -\left[(\rho-1)\alpha_0 + \frac{g}{h} \right] \begin{Bmatrix} \cos(\alpha_0\xi) \\ \sin(\alpha_0\xi) \end{Bmatrix} \pm \left[\alpha_0\xi + \frac{2(\rho-1)\xi}{h} \right] \begin{Bmatrix} \sin(\alpha_0\xi) \\ \cos(\alpha_0\xi) \end{Bmatrix} \right\}. \tag{A17b}$$

In the above

$$g = (\rho-1)^2 - \xi^2 \tag{A18a}$$

$$h = (\rho-1)^2 + \xi^2. \tag{A18b}$$

For $\rho = 1$, the integrals appearing in eqns (A5b), (A6b) and (A15) are recognized as the cosine and sine integrals, defined respectively as [13]

$$Ci(\alpha_0\xi) = -\int_{\alpha_0}^{\infty} \frac{\cos \alpha\xi}{\alpha} d\alpha \tag{A19a}$$

$$si(\alpha_0\xi) = -\int_{\alpha_0}^{\infty} \frac{\sin \alpha\xi}{\alpha} d\alpha. \tag{A19b}$$

An identical approach is used for the case of the axi-symmetric torsional loads. It has been pointed out that the expression appearing in the present solution for such torsional loads is a degenerate case of the solution of the corresponding moving torsional load problem given in [4] when q is taken as unity in the previous problem. Results for $S^{(2)}$ for the present case may be obtained from the expressions given in the appendix of [4] upon setting $q = 1$ and are therefore not repeated here.